



HAL
open science

Tellurite-based core-clad dual-electrodes composite fibers

Clément Strutynski, Frédéric Desevedavy, A. Lemièrè, Jean-Charles Jules, Grégory Gadret, Thierry Cardinal, Frédéric Smektala, Sylvain Danto

► **To cite this version:**

Clément Strutynski, Frédéric Desevedavy, A. Lemièrè, Jean-Charles Jules, Grégory Gadret, et al.. Tellurite-based core-clad dual-electrodes composite fibers. *Optical Materials Express*, 2017, 7 (5), pp.1503-1508. 10.1364/OME.7.001503. hal-01537575

HAL Id: hal-01537575

<https://hal.science/hal-01537575>

Submitted on 30 Jul 2020

HAL is a multi-disciplinary open access archive for the deposit and dissemination of scientific research documents, whether they are published or not. The documents may come from teaching and research institutions in France or abroad, or from public or private research centers.

L'archive ouverte pluridisciplinaire **HAL**, est destinée au dépôt et à la diffusion de documents scientifiques de niveau recherche, publiés ou non, émanant des établissements d'enseignement et de recherche français ou étrangers, des laboratoires publics ou privés.

Tellurite-based core-clad dual-electrodes composite fibers

C. STRUTYNSKI,^{1,2} F. DESEVEDAVY,² A. LEMIERE,² J.-C. JULES,² G. GADRET,² T. CARDINAL,¹ F. SMEKTALA,² AND S. DANTO^{1*}

¹*Institute of Chemistry of the Condensed Matter of Bordeaux, Chemistry Department (ICMCB), University of Bordeaux, 87 Doctor Schweitzer Avenue, 33608 Pessac, France*

²*Laboratoire Interdisciplinaire Carnot de Bourgogne, ICB UMR 6303 CNRS-Université de Bourgogne Franche-Comté, 9 Avenue Alain Savary, 21078 Dijon, France*

**sylvain.danto@u-bordeaux.fr*

Abstract: Tailored tellurite-glasses possess excellent thermo-viscous ability and linear/nonlinear optical properties. Here, bringing together the merits of these materials with fiber optic technology, we report on the first tellurite-based core-clad dual-electrode composite fiber made by direct, homothetic preform-to-fiber thermal co-drawing. The rheological and optical properties of the selected glasses allow both to regulate the metallic melting flow and to manage the refractive index core/clad waveguide profile. We demonstrate the electrical continuity of the electrodes over meters of fiber. We believe the drawing of architectures merging electrical and optical features in a unique elongated wave-guiding structure will enable to develop new in-fiber functionalities based on hybrid electric/optic nonlinear effects.

© 2017 Optical Society of America

OCIS codes: (060.2280) Fiber design and fabrication; (060.4370) Nonlinear optics, fibers; (160.2750) Glass and other amorphous materials.

References and links

1. N. Myrén, H. Olsson, L. Norin, N. Sjödin, P. Helander, J. Svennebrink, and W. Margulis, "Wide wedge-shaped depletion region in thermally poled fiber with alloy electrodes," *Opt. Express* **12**(25), 6093–6099 (2004).
2. K. Lee, P. Hu, J. L. Blows, D. Thorncraft, and J. Baxter, "200-m optical fiber with an integrated electrode and its poling," *Opt. Lett.* **29**(18), 2124–2126 (2004).
3. Z. Lian, M. Segura, N. Podoliak, X. Feng, N. White, and P. Horak, "Nanomechanical optical fiber with embedded electrodes actuated by joule heating," *Materials (Basel)* **7**(8), 5591–5602 (2014).
4. W. Q. Zhang, S. Manning, H. Eboroff-Heidepriem, and T. M. Monro, "Lead silicate microstructured optical fibres for electro-optical applications," *Opt. Express* **21**(25), 31309–31317 (2013).
5. S. Manning, "A study of tellurite glasses for electro-optic optical fibre devices." Ph.D. dissertation, (2011).
6. F. Sorin, A. F. Abouraddy, N. Orf, O. Shapira, J. Viens, J. Arnold, J. D. Joannopoulos, and Y. Fink, "Multimaterial photodetecting fibers: a geometric and structural study," *Adv. Mater.* **19**(22), 3872–3877 (2007).
7. S. Danto, F. Sorin, N. D. Orf, Z. Wang, S. A. Speakman, J. D. Joannopoulos, and Y. Fink, "Fiber field-effect device via in situ channel crystallization," *Adv. Mater.* **22**(37), 4162–4166 (2010).
8. M. El-Amraoui, J. Fatome, J. C. Jules, B. Kibler, G. Gadret, C. Fortier, F. Smektala, I. Skripitchev, C. F. Polacchini, Y. Messaddeq, J. Troles, L. Brilland, M. Szpulak, and G. Renversez, "Strong infrared spectral broadening in low-loss As-S chalcogenide suspended core microstructured optical fibers," *Opt. Express* **18**(5), 4547–4556 (2010).
9. I. Savellii, J. Jules, G. Gadret, B. Kibler, J. Fatome, M. El-Amraoui, N. Manikandan, X. Zheng, F. Désévéday, J. Dudley, J. Troles, L. Brilland, G. Renversez, and F. Smektala, "Suspended core tellurite glass optical fibers for infrared supercontinuum generation," *Opt. Mater.* **33**(11), 1661–1666 (2011).
10. I. Savellii, O. Mouawad, J. Fatome, B. Kibler, F. Désévéday, G. Gadret, J.-C. Jules, P.-Y. Bony, H. Kawashima, W. Gao, T. Kohoutek, T. Suzuki, Y. Ohishi, and F. Smektala, "Mid-infrared 2000-nm bandwidth supercontinuum generation in suspended-core microstructured sulfide and tellurite optical fibers," *Opt. Express* **20**(24), 27083–27093 (2012).
11. O. Mouawad, J. Picot-Clément, F. Amrani, C. Strutynski, J. Fatome, B. Kibler, F. Désévéday, G. Gadret, J.-C. Jules, D. Deng, Y. Ohishi, and F. Smektala, "Multi-octave midinfrared supercontinuum generation in suspended-core chalcogenide fibers," *Opt. Lett.* **39**(9), 2684–2687 (2014).
12. C. Strutynski, J. Picot-Clément, A. Lemiere, P. Froidevaux, F. Désévéday, G. Gadret, J.-C. Jules, B. Kibler, and F. Smektala, "Fabrication and characterization of step-index tellurite fibers with varying numerical aperture for near- and mid-infrared nonlinear optics," *J. Opt. Soc. Am. B* **33**(11), D12–D18 (2016).

13. S. Kedenburg, C. Strutynski, B. Kibler, P. Froidevaux, F. Désévéday, G. Gadret, J.-C. Jules, T. Steinle, F. Mörz, A. Steinmann, H. Giessen, and F. Smektala, "High-repetition-rate mid-infrared supercontinuum generation from 1.3-5.3 μm in robust step-index tellurite fibers," *J. Opt. Soc. Am. B*, submitted.
14. A. Canales, X. Jia, U. P. Froriep, R. A. Koppes, C. M. Tringides, J. Selvidge, C. Lu, C. Hou, L. Wei, Y. Fink, and P. Anikeeva, "Multifunctional fibers for simultaneous optical, electrical and chemical interrogation of neural circuits in vivo," *Nat. Biotechnol.* **33**(3), 277–284 (2015).

1. Introduction

The development of fully integrated all-fiber optical systems is of tremendous technological interest in photonics. The progressive shift from free-space optical components towards fiber optical equivalents would allow for more compact, harsh, electromagnetic immune, cheaper devices. Here we propose to design a new class of glass/metal composite fibers for all-guided optical-electrical signals. Indeed, the development of fibers combining both optical waveguide properties and simultaneous in-fiber electrical excitation could provide numerous innovative signal-processing, sensing or imaging functionalities. To succeed continuous metallic electrodes running along the fiber axis have to be implemented following specific designs to match a proper impedance and to properly deliver electric energy. Crystalline materials, such as metallic compounds, are characterized by an abrupt drop in their viscosities at the melting temperature, which makes them incompatible with thermal drawing. Various methods have been developed recently, mostly on silica-based fibers as it still vastly dominates fiber-optics market, to alleviate this limitation. Margulis *et al.* fabricated silica-based glass/metal optical fibers for electro-optical switch operation based on Kerr effect [1]. Here high pressure was used to fill the longitudinal capillary twin-holes of a tens-of-meters-long core-clad fiber structure with a molten Sn-based alloy. Alternatively single-electrode core-clad germano-silica optical fibers were manufactured by feeding the preform with a 50- μm tungsten wire coil during the drawing [2]. In a different approach, Lian *et al.* combined stack-and-draw and co-draw techniques to produce dual-cores multiple-electrodes fibers [3]. In the latter case, a low- T_g lead-silicate glass ($T_g = 592\text{ }^\circ\text{C}$) was used, enabling a co-drawing at 730 $^\circ\text{C}$. Despite its technological interest, silica exhibit several limitations as compared with low- T_g glass systems (tellurites, chalcogenides...). Firstly, a fundamental limitation to poling efficiency is the values of the induced $\chi^{(2)}$, which is at least an order-of-magnitude lower than for other non-silica glass materials, as well as the low $\chi^{(3)}$. In addition, low- T_g glass systems exhibit moderate processing temperatures, allowing for a larger panel of potential metals to be co-drawn with. Monro *et al.* identified tellurite glasses as being especially suitable for electro-optical fiber devices, owing to their large nonlinear coefficients and drawing ability [4,5]. Here post-drawing liquid metal injection was employed for providing optical fibers with internal electrodes. Finally, beside implementing electrodes for exploiting nonlinear effects, the direct glass + metal fiber co-drawing method was developed to produce glass/metal/polymer fibers for photo-detection, piezoelectricity and so on [6,7].

Recently we have developed an original drilling approach for preparing holey glass preforms with a variety of geometrical patterns in view of micro-structured fiber drawing [8]. We used the method for fabricating micro-structured soft- T_g glass fibers for supercontinuum generation [9–11]. The drilling approach is expanded here to manufacture glass/metal composite fibers through the scalable process of thermal drawing. A glass macroscopic preform is drilled and filled with a metallic wire. Then the glass/metal preform is elongated in a homothetic fashion through localized thermal heating in meters-long core/clad fibers with embedded electrodes. Tellurium oxide glasses are especially suitable for this study owing to their large 3rd-order nonlinear coefficient and their wide optical transparency from the visible up to 6 μm . Specifically we have selected glasses in the $\text{TeO}_2\text{-ZnO-Na}_2\text{O}$ (TZN) system because of their high stability against crystallization [10]. First, we assessed the glass/metal co-drawing method through the fabrication of a single-electrode tellurite fiber. Then, a more sophisticated core-clad dual-electrodes fiber profile was explored. Thermal analysis, scanning electron microscopy and electrical measurements were used to establish the conservation and continuity of the electrodes along the fiber devices.

2. Experimental details

The glasses were melted using the standard melt-quench technique (see Table 1 for compositions). High-purity precursors were weighted in powder forms and mixed together in a platinum crucible. The mix was ramped up ($10\text{ }^{\circ}\text{C}\cdot\text{min}^{-1}$) at $850\text{ }^{\circ}\text{C}$ and then kept at this temperature for 4 hours. Following preforms were produced by casting the glass in a cylindrical brass mold annealed at $T_g-10\text{ }^{\circ}\text{C}$ for 12 hours. Quasi single-mode tellurite fibers were manufactured by combination of the build-in casting and rod-in-tube techniques, as described more extensively in [12]. The method was extended to prepare glass/metal composite fibers. The fabrication of single-electrode fibers started by the drilling of a mono-index glass rod and insertion of a metallic wire. The fabrication of core/clad dual-electrodes fiber proceeded in two steps. Firstly, we fabricate a large-core step-index preform from two different glasses (core and clad) by build-in casting and stretch it down to $800\text{-}\mu\text{m}$ thin capillary rods. It is then inserted in mechanically drilled 16-mm outer diameter glassy jacket tube, along with two metallic wires. The thermal co-drawing ability of the materials was assessed using a dedicated 3-meters-high optical fiber draw tower. The preform was slowly fed into the furnace and the temperature was gradually increased up to $\sim 400\text{ }^{\circ}\text{C}$. The glass was brought to its softening temperature regime while the drawing parameters were continuously monitored to produce the targeted fiber diameter.

Thermal analysis was performed by differential thermal analysis (DSC 2920 TA Instruments) on 20 mg samples. Characteristic temperatures were measured as the inflection point of the endotherm at a heating rate of $10\text{ }^{\circ}\text{C}/\text{min}$ (precision $\pm 2\text{ }^{\circ}\text{C}$ for T_g measurements). The electrical measurements were carried out with a 447097 expert line multi-meter on meters-long fiber samples. Both cleaved ends of the fiber were coated with silver paint to make electrical contacts. After the measurements, the electrodes size was checked every 20 cm by optical microscopy. We measured refractive index on polished glass slabs at 1550 nm using a homemade prism (TiO_2) coupler refractometer. Fiber profile and chemical composition were checked on cleaved carbon-coated samples thanks to Scanning Electron Spectroscopy (SEM) and Energy Dispersive Spectroscopy (EDS).

3. Results and discussion

3.1 Materials selection

The selected glass compositions are specified in Table 1. It consists of the glasses $80\text{TeO}_2\text{-}10\text{ZnO-}10\text{Na}_2\text{O}$ (TZN), $60\text{TeO}_2\text{-}5\text{ZnO-}20\text{Na}_2\text{O-}15\text{GeO}_2$ (TZNG) and $80\text{TeO}_2\text{-}5\text{ZnO-}10\text{Na}_2\text{O-}5\text{ZnF}_2$ (TZNF) [12]. The TZN, TZNG and TZNF have similar glass transition temperatures (respectively $285\text{ }^{\circ}\text{C}$, $272\text{ }^{\circ}\text{C}$ and $282\text{ }^{\circ}\text{C}$) and show no discernable crystallization events below $400\text{ }^{\circ}\text{C}$, which attests for their suitability for thermal drawing. The melting temperature of the metal has to be below the drawing temperature of the preform to be suitable for co-drawing. Here we have selected the alloy $\text{Au}_{80}\text{Sn}_{20}$ ($T_m = 282\text{ }^{\circ}\text{C}$).

Table 1. Investigated materials and their key properties

Materials	Composition (mol%)		T_g [$\pm 2\text{ }^{\circ}\text{C}$]	T_x [$\pm 2\text{ }^{\circ}\text{C}$]	T_m [$\pm 2\text{ }^{\circ}\text{C}$]	n (@ 1550 nm) [± 0.001]
<i>Single-electrode tellurite fiber</i>						
TZN	$80\text{TeO}_2\text{-}10\text{ZnO-}10\text{Na}_2\text{O}$	Cladding	$285\text{ }^{\circ}\text{C}$	$>400\text{ }^{\circ}\text{C}$	-	1.995
AuSn	$\text{Au}_{80}\text{Sn}_{20}$	Electrode	-	-	$280\text{ }^{\circ}\text{C}$	-
<i>Dual-electrode core-clad tellurite fiber</i>						
TZNG	$60\text{TeO}_2\text{-}5\text{ZnO-}20\text{Na}_2\text{O-}15\text{GeO}_2$	Cladding	$272\text{ }^{\circ}\text{C}$	$>400\text{ }^{\circ}\text{C}$	-	1.867
TZNF	$80\text{TeO}_2\text{-}5\text{ZnO-}10\text{Na}_2\text{O-}5\text{ZnF}_2$	Core	$282\text{ }^{\circ}\text{C}$	$>400\text{ }^{\circ}\text{C}$	-	1.989
AuSn	$\text{Au}_{80}\text{Sn}_{20}$	Electrodes	-	-	$280\text{ }^{\circ}\text{C}$	-

3.2 Single-electrode tellurite fiber

Our first experiment involved the drawing of a single-electrode TZN glass preform. The preform consists of a cylindrical macroscopic glass rod ($\Phi_{\text{Preform}} = 16$ mm), drilled ($\Phi_{\text{Hole}} = 0.8$ mm) and fed with an AuSn wire. Following it is softened at elevated temperatures and stretched down into meters-long fiber with diameter ~ 200 μm . Cross-sectional view of the fiber is depicted on Fig. 1(a). Comparative differential scanning calorimetry were carried out in order to assess deviations of the characteristic temperatures of the materials induced by the co-drawing process. Figure 1(b) shows the DSC trace of the TZN bulk glass, the Au-Sn bare electrode and of a complete section of TZN single-electrode composite fiber.

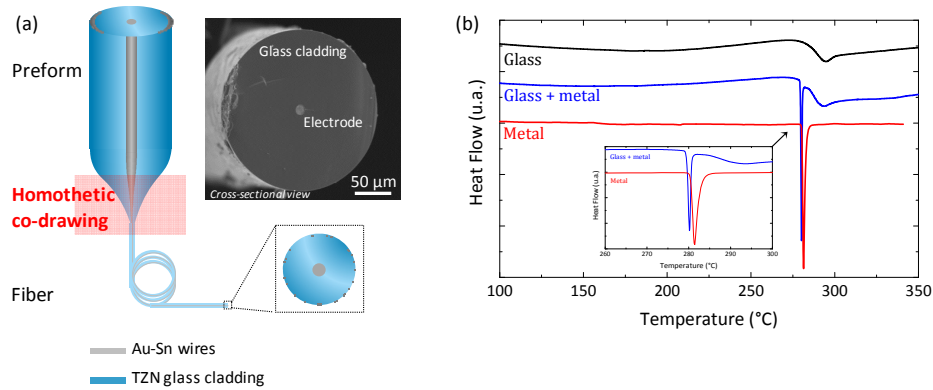


Fig. 1. (a) Homothetic preform-to-fiber glass/metal co-drawing; SEM micrograph of the fiber cross-section (b) DSC traces of the TZN bulk glass, $\text{Au}_{80}\text{Sn}_{20}$ bare electrode and glass/metal composite fiber.

The DSC trace of the bare TZN glass exhibits an endothermic event at $T_{\text{g TZN}} = 285$ $^{\circ}\text{C}$, corresponding to its glass transition temperature, while the $\text{Au}_{80}\text{Sn}_{20}$ alloy shows a sharp melting peak at $T_{\text{m Au-Sn}} = 280.5$ $^{\circ}\text{C}$. If now considering the DSC trace of the glass/metal composite fiber, we have $T_{\text{g TZN}} = 285$ $^{\circ}\text{C}$ and $T_{\text{m Au-Sn}} = 279.6$ $^{\circ}\text{C}$. DSC analysis shows no deviation in the positioning of the glass transition temperature of the TZN glass. We note however a slight decrease ($\Delta T_{\text{m Au-Sn}} = -0.9$ $^{\circ}\text{C}$) of the melting peak of the alloy once drawn into fiber. We believe it might emanate from a chemical contamination occurring at the interface between the two materials during the drawing process.

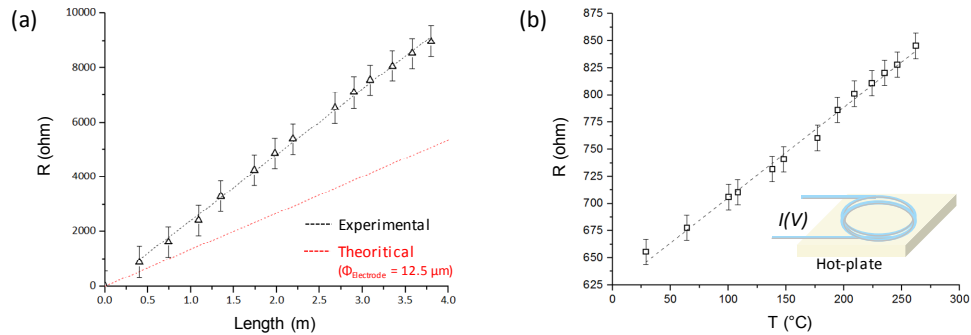


Fig. 2. Electrical characterization of the glass/metal fiber (a) Resistance $R_{\text{Fiber}} = f(L_{\text{Fiber}})$ at $T = 25$ $^{\circ}\text{C}$ (b) Resistance $R_{\text{Fiber}} = f(T)$ for $L_{\text{Fiber}} = 7$ meters.

In order to verify the continuity of the electrode we performed electrical measurements, both as a function of fiber length in Fig. 2(a) and of temperature in Fig. 2(b). On Fig. 2(a) we plot $R_{\text{Fiber}} = f(L_{\text{Fiber}})$, the electrical resistance of the fiber as a function of its length, at $T = 25$

°C. The I - V resistance characteristics of the fiber shows a clear Ohmic response (black line). Knowing the resistivity of $\text{As}_{80}\text{Sn}_{20}$ ($\rho_{\text{As}_{80}\text{Sn}_{20}} \sim 16.4 \cdot 10^{-8} \Omega \cdot \text{m}$) and the diameter of the electrode ($\Phi_{\text{Electrode}} = 12.5 \mu\text{m}$) we calculated the expected resistance with length of the electrode (red line). We observe that the measured resistance is approximately twice superior to the theoretical one. This discrepancy might be due to a contamination of the metallic electrode or to the generation of grain boundaries within the metal during drawing. Further investigations are in progress to elucidate the origin of this phenomenon, which has to be related with the slight variation of the alloy's melting peak observed on Fig. 1. On Fig. 2(b) we plot $R_{\text{Fiber}} = f(T)$ with $L_{\text{Fiber}} = 7$ meters. The I - V resistance characteristics of the fiber shows an Ohmic response typical of a metallic behavior.

3.3 Dual-electrode core-clad tellurite fiber

The thermo-viscous flowing ability of the tellurite glasses allows for the fabrication of single-electrode composite fiber. Now we proceed to overtake a more sophisticated task, namely the direct preform-to-fiber drawing of a core-clad dual-electrodes fiber, as outlined on Fig. 3. Three holes are drilled on a TZNG glass preform, in its center and from either side of the center ($\Phi_{\text{Preform}} = 16 \text{ mm}$, $\Phi_{\text{Hole}} = 0.8 \text{ mm}$). The central hole hosts a TZNF-TZNG step-index capillary while the two axial ones host one Au-Sn wire each, as displayed in Fig. 3(a). The whole composite structure is then stretched down into a tellurite/germano-tellurite core-clad structure, as shown in Fig. 3(b). The micrographs of the fiber (cross-sectional view: SEM; longitudinal view: optical microscope $\times 10$) reveal a proper transfer of the geometry of the preform into fiber.

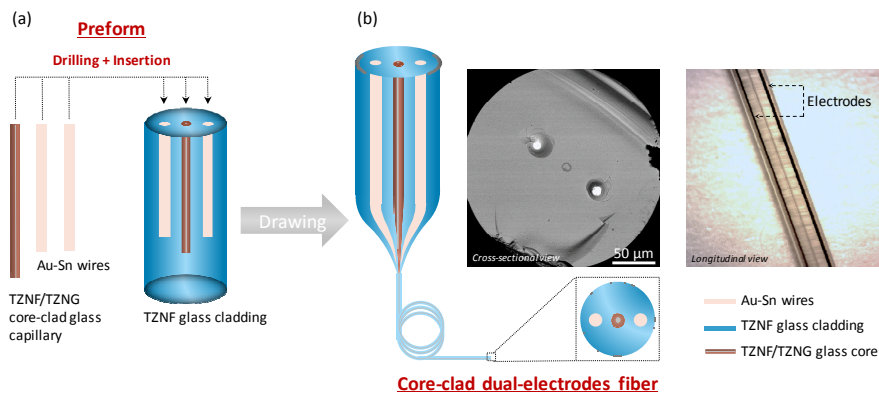


Fig. 3. Homothetic dual-electrodes core-clad co-drawing (a) Design of the preform (b) Scheme of the drawing, SEM micrographs of the fiber (cross-sectional view: SEM ; longitudinal view: optical microscope $\times 10$).

SEM micrograph on Fig. 4(a) depicts the cross-sectional view of the fiber (magnification $\times 250$). In order to detect stoichiometric deviation or inter-diffusion between the glass and electrodes we scan the sample by EDS along the electrode-core-electrode line (for clarity we show Te, Ge, Au and Sn measurements only). The concentration variation of the elements along the electrode-core-electrode scanned line is in good agreement with the expected compositions.

Following we verified how light propagates into the step-index dual-electrode fiber. A light beam ($\lambda = 1.55 \mu\text{m}$) was injected into a 1-meter-long fiber sample using a FTIR spectrometer. We imaged the output beam intensity distribution using a microscope objective and a CCD camera, as displayed in Fig. 4(b). First we confirm the propagating property of the glass core (and in a lesser extend of the cladding due to the lack of clad depletion by means of a metallic coating). Besides, the two dark circular spots from either side of the illuminated core highlight the presence of the metallic electrodes within the cladding.

Noteworthy, we demonstrated on the highly nonlinear step-index tellurite fiber architecture proposed here very low background propagation losses ($\sim 0.5 \text{ dB.m}^{-1}$) for OH-free fibers [12] and a dispersion engineering allowing two octaves supercontinuum generation from $1.3 \mu\text{m}$ to $5.3 \mu\text{m}$, hence reaching the multi-phonon edge of the matrix [13].

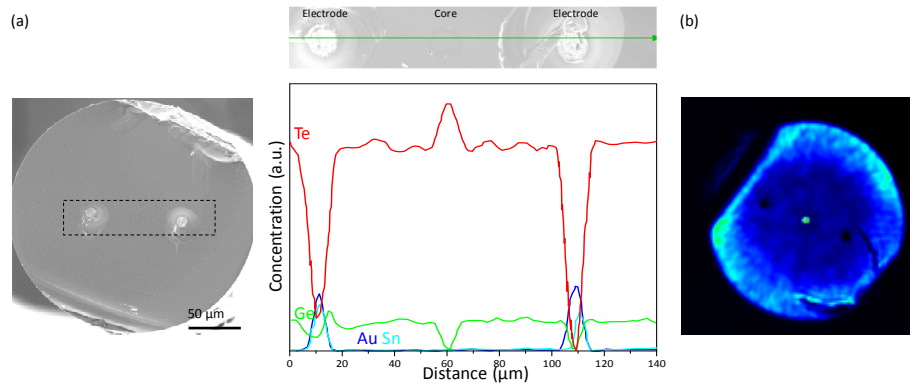


Fig. 4. Tellurite-based dual-electrodes fiber (a) SEM micrograph of the whole fiber cross-section and EDS analysis for Te, Sn and Au elements across the electrode-core-electrode line (b) Light transmission at $1.55 \mu\text{m}$ ($L_{\text{Fiber}} = 1 \text{ m}$).

Hence we demonstrate the manufacturing of tellurite-based dual-electrodes core-clad composite fibers. Our fabrication approach is based on the drilling of a centimeter-scale preform followed by its stretch down. It allows to create fiber cross-sections with complex geometrical patterns incorporating various materials. The metal compound, intrinsically incompatible with thermal drawing, is embedded into the high-viscosity glass cladding, which acts as a support to restrict the flow of the molten phase. Following this procedure, we produced continuous metallic electrodes running parallel to the optical core over meters of fiber. The reduction of the lateral dimensions of the preform during its drawing brings the glass and metal domains in intimate contact over meters. Currently in progress is the refinement of our fabrication process in order to increase the length, number and conductivity of the electrodes to enhance the electric field. Future work will consist in developing a deeper understanding of the chemistry involved at the glass/metal interface during the drawing to alleviate potential issues due to inter-diffusion of species during drawing. A potential application of tellurite glass/metal composite fibers could be electro-endoscopes for medical treatment. Recent advances have permitted neural stimulation/recording activity with increasing resolution [14].

4. Summary

Here we propose glass/metal composite fibers fabricated from soft- T_g tellurite glasses. Our approach relies on the simultaneous drawing of tellurite glasses with embedded metallic electrodes. The rheological and optical properties of the selected glasses allow to manage both the control of metallic flow during the fiber drawing and the refractive index profile of the core/clad waveguide. The ability to insert materials with disparate optical and electrical properties within glass fibers opens new opportunities for increasing the complexity of fiber structures. Controlling both the light propagation features and a simultaneous DC/microwave excitation along fiber axis could lead to innovative in-fiber functionalities based on hybrid electric/optic nonlinear effects.

Funding

French National Research Agency (ANR Holigrade #40611/ANR PhosFyb #50526); Programme IdEx at the University of Bordeaux; Cluster of excellence LAPHIA; Conseil Régional de Bourgogne; Région Nouvelle Aquitaine.